Experimental Measurements of Benzene Oxidation in Supercritical Water

Joanna L. DiNaro, Jefferson W. Tester, and Jack B. Howard
Dept. of Chemical Engineering and Energy Laboratory, Massachusetts Institute of Technology, 77 Massachusetts Ave., Rm. E40-455, Cambridge, MA 02139

Kathleen C. Swallow
Dept. of Chemistry and Engineering, Merrimack College, North Andover, MA 01845

Oxidation and hydrolysis reactions of benzene in supercritical water were investigated thoroughly using experimental measurements. Little to no reaction occurred without oxygen at temperatures between 530 and 625°C for residence times up to 6 s. Oxidation reactions were studied at temperatures ranging from 479 to 587°C, pressures of 139 to 278 bar, reactor residence times from 3 to 7 s, and with varying initial benzene concentrations from 0.4 to 1.2 mmol/L and oxygen concentrations from 40% of oxygen demand to 100% excess oxygen. To a 95% level of statistical confidence, the oxidation rate was found to be of 0.04 $\pm$ 0.07 order in benzene, 0.17 $\pm$ 0.05 order in oxygen, and 1.4 $\pm$ 0.1 order in water, with an activation energy of 270 $\pm$ 10 kJ/mol. The primary oxidation product at all reaction conditions studied was carbon dioxide. Other important oxidation products were carbon monoxide, phenol, and methane. Trace levels of additional light hydrocarbon gases and single- and multi-ringed aromatic species were also detected under some conditions.

Introduction

Supercritical water oxidation (SCWO) typically refers to a waste treatment or remediation process that derives its effectiveness from the unique solvent properties of water well above its critical point of 221 bar and 374°C. When organic compounds and oxygen are brought together in supercritical water (SCW), the oxidation of the organic to carbon dioxide and water is rapid and complete. Heteroatoms such as Cl, S, and P are converted to their corresponding mineral acids (HCl, H_2SO_4, and H_3PO_4) and can be neutralized using a suitable base. If any nitrogen is present, either introduced with the water or if air is used as the source of O_2, the resulting product is N_2 or N_2O (Killilea and Swallow, 1992). NO_x gases, typical undesired byproducts of combustion processes, are not formed because the temperature is too low for these oxidation pathways to be favored. Practical SCWO processes usually operate between 450 and 600°C and 250 to 280 bar. Detailed reviews of the technology can be found in Modell (1989), Tester et al. (1993a), Gloyna and Li (1995), and Tester and Cline (1999).

Our research emphasizes investigating the hydrolysis (reaction in the absence of oxygen) and oxidation of simple organic compounds in supercritical water. Certain specific organic compounds, referred to as ''model compounds,'' were selected for study because they either are the rate-limiting steps in the oxidation of more complex compounds, are simulants for hazardous waste compounds, represent wide classes of organic wastes, or are themselves characteristic waste compounds. To that end, comprehensive studies involving measuring oxidation and hydrolysis rates were performed at MIT on carbon monoxide (Helling and Tester, 1987, 1988; Holgate et al., 1992; Holgate and Tester, 1994a,b), ethanol (Helling and Tester, 1988), ammonia (Helling and Tester, 1988; Webley et al., 1990, 1991), methane (Webley and Tester, 1991), methanol (Webley and Tester, 1989; Webley et al., 1990, 1991; Tester et al., 1993b), hydrogen (Holgate and Tester, 1993, 1994a,b), glucose (Holgate et al., 1995), acetic acid (Meyer et al., 1995), thiodiglycol (Lachance et al., 1999), and methylene chloride (Marrone et al., 1995, 1998a,b; Salvatierra et al., 1999). Many of these model compounds exhibited overall first-order kinetic behavior under oxidative conditions. Re-

Correspondence concerning this article should be addressed to J. W. Tester.

cently, methanol oxidation kinetics were reinvestigated for the purposes of studying mixing effects, evaluating the use of hydrogen peroxide as an alternative oxidant, and performing a direct comparison of kinetic data measured in our lab with that independently gathered at Sandia National Laboratories (Phenix et al., 2000; Vogel et al., 2000).

Expanding upon the research focusing on measuring SCWO reaction kinetics of model compounds, a comprehensive experimental investigation of the homogeneous SCWO of benzene, a representative model aromatic compound, was undertaken. In addition to being classified as a hazardous chemical, a known human carcinogen, and an environmental contaminant, the single aromatic ring of benzene is the building block for polyaromatic hydrocarbons (PAHs) and substituted aromatic compounds. This study of the SCWO of benzene contributes to the collective knowledge of reaction kinetics and the advancement of the SCWO technology by providing both an understanding of the kinetics of benzene itself and lending insight as to the reactive behavior of a more general class of chemicals.

A detailed review by Savage et al. (1995) covers reactions in supercritical fluids, including water, and the recently published subsequent review (Savage, 1999) surveys organic reactions in SCW. Here we review the relevant literature focusing on the SCWO of aromatic compounds.

Benzene and many other aromatic compounds were proven amenable to treatment by SCWO (Thomason et al., 1990). Ding et al. (1995a,b) reported a few measurements for homogeneous benzene, phenol, and 1,3-dichlorobenzene oxidation in their flow system, but their research emphasized catalytic SCWO. In all cases CO_2 was the major product, CO was not detected, and significant yields of dimers, single-ring aromatic species, and organic acids were measured. Of the three aromatics studied, phenol was the easiest to oxidize, and conversion with a high selectivity to CO_2 was achieved without catalyst at only 390°C and 241 bar with a 13 s residence time. Statistically significant oxidation of benzene at 241 bar and a 13 s residence time did not occur until 450°C.

Although only limited data are available for benzene, the situation for other aromatics is better. For example, the early investigations of Savage et al. at the University of Michigan focused on phenol SCWO (Thornton and Savage, 1990, 1992a,b; Thornton et al., 1991; Li et al., 1992; Gopalan and Savage, 1995). Later studies measured the oxidation of the *o*-, *m*-, and *p*- isomers of phenols with $-CH_3$ (cresols) and —CHO (hydroxybenzaldehydes) substituent groups (Martino et al., 1995; Martino and Savage, 1997) and the thermolysis and oxidation of the *o*-, *m*-, and *p*- isomers of phenols with $-C_2H_5$ (ethylphenols), $-COCH_3$ (hydroxyacetophenones), $-NO_2$ (nitrophenols), $-OCH_3$ (methoxyphenols), and —OH (benzenediols) substituent groups (Martino and Savage, 1999a,b). Levec and coworkers at the University of Ljubljana in Slovenia performed complementary investigations to those of Savage et al., studying both the homogeneous (Krajnc and Levec, 1996) and catalytic (Krajnc and Levec, 1997) SCWO of phenol. Phenol oxidation was also studied by Koo et al. (1997), Rice and Steeper (1998), and Oshima et al. (1998). Also investigated were the catalyzed and uncatalyzed SCWO of 1,4-dichlorobenzene (Jin et al., 1992), the homogeneous SCWO of hydroquinone (Thammanayakatip et al., 1998), the catalyzed and uncatalyzed SCWO of *p*-chlorophenol (Yang and Eckert, 1988), and the homogeneous (Crain et al., 1993) and catalytic (Aki and Abraham, 1999) SCWO of pyridine.

Several similarities exist between the preceding investigations on the reactions of aromatic compounds in supercritical water. Carbon dioxide is the highest yielding product in all investigations, and even dominates over CO at very low conversions of the aromatic reactant and at very short reactor residence times. The high yields of CO_2 at short residence times and temperatures too low for the oxidation of CO to CO_2, based on the previous investigation of CO SCWO kinetics (Holgate et al., 1992), indicate that CO_2 is formed by a pathway other than through the direct oxidation of CO. A second similarity is the presence of single-ringed aromatic species (primarily benzenediols and benzoquinones). Oxidation of the aromatic compounds appears to proceed by parallel, consecutive pathways: one forming dimers and the other forming single-ring products. Higher temperatures and higher levels of oxygen appear to favor the single-ring products (the benzoquinones and benzenediols) over the dimers.

None of the studies cited provide intrinsic kinetic data for the hydrolysis or oxidation of benzene in supercritical water. Thus, we undertook an aggressive experimental program to measure the rates of these reactions as a function of the reactor operating variables (temperature, initial organic and oxidant concentrations, residence time, and pressure or density) and correlate the data in the form of a regressed global rate expression.

Experimental and Analytical Methods

All experiments were conducted in a modified version of the bench-scale, tubular plug-flow reactor that has been used for all previous experimental studies in this laboratory (Holgate and Tester, 1993; Marrone et al., 1995). Modifications to the original system include: (1) replacement of the feed pumps; (2) redesign of the preheating system; (3) redesign of the cross at the reactor entrance in which the organic and oxidant streams are mixed (Phenix et al., 2001); and (4) introduction of hydrogen peroxide for the *in situ* generation of molecular oxygen in the preheater (Phenix et al., 2001). The reactor system is briefly described below.

Separate organic and oxidant feed solutions were prepared. A.C.S. grade benzene (EM Guaranteed Reagent) was used as received to prepare a saturated aqueous benzene feed solution. Hydrogen peroxide (H_2O_2), which decomposes in the preheating section of the reactor system producing oxygen and water, was used as the oxygen source in the majority of the oxidation experiments. To prepare an H_2O_2 feed solution, a 30 wt % aqueous solution of A.C.S. grade H_2O_2 (Mallinckrodt; Aldrich Chemical Company) was used as received and diluted with deionized water to the desired concentration. Experiments performed using dissolved oxygen in place of H_2O_2 confirmed that benzene oxidation kinetics were independent of the oxidant choice (see Phenix et al., 2001 for a comparison of methanol oxidation rates using either oxidant). The organic and oxidant feed were pressurized to the reactor pressure (typically 246 bar) and delivered to the system via two independent, digital HPLC pumps (Rainin, SD-200) that

replaced the older-model pumps (LDC Analytical, minipump model 2396) used by previous investigators at MIT.

The pressurized organic and oxidant feeds were preheated to operating temperature before the two feeds were mixed in a modified cross at the reactor entrance. The preheater system consists of two subsections: a direct ohmic preheating section followed by preheating coils located in the fluidized sandbath (Techne, FB-08) that houses the reactor. The direct ohmic heating (DOH) system separately heats the aqueous organic and oxidant feeds to the reaction temperature using resistive heating and replaces the reheater sandbath used by earlier investigators (Holgate and Tester, 1993; Marrone et al., 1995). Heating in the DOH section is accomplished by applying a voltage across independent 9.5-m lengths of 1/16-in. (1.6-mm) OD $\times$ 0.01-in. (0.25-mm) wall Hastelloy (HC-276) tubing. Temperature regulation of the DOH system is accomplished by controlling the applied voltage levels. The last approximately 0.5 m of the 9.5-m DOH preheating coils, situated just before the preheaters drop into the sandbath, are traced with heat tape. To provide heating to the approximately 30-cm section of preheater tubing on each of the feed streams just after the DOH section and before the feeds enter the sandbath, resistive cable heaters (Watlow, p/n 62H24A6X, 1/16 in. (1.6 mm) O.D. $\times$ 2 ft (61 cm) long, 10 V, 240 W max.) are wrapped around the tubing with power controlled by variable transformers. Once the organic and oxidant streams enter the sandbath, each stream passes through an additional 5.2 m coiled length of 1/16-in. (1.6-mm) OD $\times$ 0.01-in. (0.25-mm) wall HC-276 tubing.

Mixing of the organic and oxidant streams is accomplished in a specially modified 1/8-in. (3.2-mm) HC-276 cross from High Pressure Equipment (p/n 60-24HF2). The feed streams enter the cross in opposed flow configuration. The internal diameters of the two arms of the cross through which the organic and oxidant feeds enter were reduced from their original 1/16 in. (1.6 mm) ID to 0.01 in. (0.25 mm) ID to increase the velocities of the organic and oxidant feeds, and thus increase the rate of mixing, by press fitting short lengths of 1/16-in. (1.6-mm) OD $\times$ 0.01-in. (0.25-mm) ID 316SS tubing into those arms. Details of the mixing cross configuration can be found in Phenix et al. (2001). A 1/16-in. Type K thermocouple is seated in the top port of the cross, and its tip extends into the fluid. The reactor itself is seated into the fourth port of the cross and is a 1/4-in. (6.35-mm) OD $\times$ 0.067-in. (1.7-mm) ID 4.71-m coiled length of Inconel 625 tubing with an internal volume of 10.71 cm^3. A second 1/16-in. Type K thermocouple is seated in an 1/8-in. (3.2-cm) HC-276 tee at the reactor exit. A 26-cm length of 1/4-in. (6.35-mm) OD $\times$ 1/16-in. (1.6-mm) ID insulated HC-276 tubing rises out of the sand and connects the reactor to the heat exchanger.

The reactor effluent enters the inner tube of a shell-and-tube heat exchanger and is immediately quenched. A spring-loaded, manual backpressure regulator (Tescom, p/n 26-3200) controls system pressure. Upon passing through the backpressure regulator, the effluent is flashed to atmospheric pressure and the two-phase effluent is separated in a gas–liquid separator. Gas samples are taken from the sampling port with a syringe, and the flow rate of the gas stream is measured using the soap-bubble flowmeter and a stopwatch. Liquid samples are collected from the liquid-effluent line, and the flow rate is measured using a Class A volumetric flask and a stopwatch.

The benzene feed solution, liquid- and gas-phase effluent were analyzed by gas chromatography (GC). During an experiment, at least five samples of the benzene feed solution and six liquid-phase samples were collected and subjected to multiple analyses on either an HP-5890 Series II GC with a flame ionization detector (FID), an HP-6890 GC with an FID, or on both GCs. On the HP-5890 GC analytes were separated on a 30-m $\times$ 530-μm $\times$ 5-μm film thickness DB-1 column (J&W Scientific) preceded by 5 m of a Restek Hydroguard retention column. The same guard column was used on the HP-6890 GC, but the main column was a 30-m $\times$ 530-μm $\times$ 1-μm film thickness DB-WAX column (J&W Scientific). Six gas-phase samples were collected per experiment. The analysis of O_2, N_2, CO, CO_2, and CH_4 was performed by GC/TCD on both the HP-5890 Series II and HP-6890 GCs using 5-ft (1.5-m) $\times$ 1/8-in. (3.2-mm) 60/80 mesh Carboxen 1000 columns connected in series through air-actuated switching valves with 8-ft (2.4-m) $\times$ 1/8-in. (3.2-mm) 60/80 mesh Molsieve 5A columns and helium carrier gas. A Perkin-Elmer Sigma 1B GC, also with a TCD but using nitrogen carrier gas and a 12-ft (3.7-m) $\times$ 1/8-in. (3.2-mm) 80/100 mesh Porapak T column connected to an 8-ft $\times$ 1/8-in. 60/80 mesh Molsieve 5A, was used for the detection of hydrogen and helium. Analysis of light hydrocarbons and gas-phase benzene was performed on a second HP-5890 Series II GC with an FID and a 15-m $\times$ 320 μm Astec Gas Pro bonded PLOT column.

Five experiments were conducted for the purpose of identifying single and multiringed aromatic products and monitoring their occurrence as a function of temperature and the initial oxygen concentration. Between 500 and 750 mL of aqueous effluent from each of these five experiments was collected, extracted with methylene chloride (CH_2Cl_2) and concentrated. The extracted, concentrated samples were analyzed for single- and multiringed aromatic species by GC/MS using EPA Method 8270C "Semivolatile Organic Compounds by GC/MS" (U.S. EPA, 1996).

Experiments Performed

A total of 7 hydrolysis and 107 oxidation experiments were conducted to characterize the reactivity of benzene in supercritical water. The hydrolysis experiments measured the conversion of benzene in the absence of oxygen. Table 1 presents the range of conditions explored in the experiments. The temperature (T), residence time (τ), initial benzene concentration ($[C_6H_6]_0$), fuel equivalence ratio (Φ), and pressure (P) were varied during these experiments. The fuel equivalence ratio is defined by

Table 1. Conditions Explored in Benzene SCW Experiments

	Oxidation Exp.	Hydrolysis Exp.
T (° C)	479–587	530–625
P (bar)	138–278	246
τ (s)	3–7	6
$[C_6H_6]_0$ (mM)	0.4–1.2	0.48–1.25
Φ	0.5–2.5	—

$$\Phi \equiv \frac{([C_6H_6]/[O_2])_{\text{initial}}}{([C_6H_6]/[O_2])_{\text{stoichiometric}}}, \quad (1)$$

such that $\Phi < 1$ indicates excess oxygen and fuel-rich conditions are signified by $\Phi > 1$. A stoichiometric level of oxygen ($\Phi = 1$) was used in the majority of the experiments in order to be consistent with previous MIT SCWO studies. A nominal operating pressure of 246 bar was selected, also for consistency purposes. This pressure is representative of those used industrially and is far enough above the critical pressure that the physical properties of water (density, dielectric strength, ion product, etc.) are not affected by small pressure fluctuations. The initial benzene concentration ($[C_6H_6]_0$), which is that at the reactor entrance, was limited by the ambient concentration of benzene in water (approximately 1800 ppm). Table 2 groups the oxidation experiments in Table 1 into four categories and indicates the variable and fixed-condition parameter values and residence-time ranges. The experimental data can be found in tabular form in DiNaro (1999).

Kinetic Results

Hydrolysis experiments

The hydrolysis experiments were conducted at 246 bar with a 6-s reactor residence time and temperatures ranging from 530°C to 625°C. Phenol was the only quantifiable, detected hydrolysis product. Although CO, CO_2, methane, ethane, ethylene, and hydrogen were also observed, their amounts were not quantified, as the gas flow rate was too low to measure (< 0.06 mL/min). No benzene conversion was detected at 530°C, and conversion at 580, 600 and 625°C was determined to be no greater than 10% and on average closer to 2% based on the effluent phenol concentration. Since, as will be discussed, benzene undergoes near complete conversion by an oxidative pathway with similar reaction conditions by a temperature of 575°C, the hydrolysis pathway did not interfere with the study of benzene oxidation kinetics.

Oxidation experiments

Temperature Variations. Temperature was varied from 479°C to 587°C at a fixed pressure of 246 bar, residence time of 6 s, initial benzene concentration of 0.6 mM, and with a stoichiometric level of oxygen. Benzene conversion as a function of reactor temperature appears in Figure 1. The error bars in this and all subsequent figures are at the 95% confidence level. Benzene oxidizes only minimally at temperatures less than 520°C. Conversion increases rapidly with temperature between 520 and 565°C and is essentially complete above 565°C. Carbon monoxide, carbon dioxide, methane, and phenol were the primary products of benzene oxidation. Figures 2 and 3 display the carbon fractions of these products along with that of unreacted benzene as a function of temperature, where carbon fraction is defined as

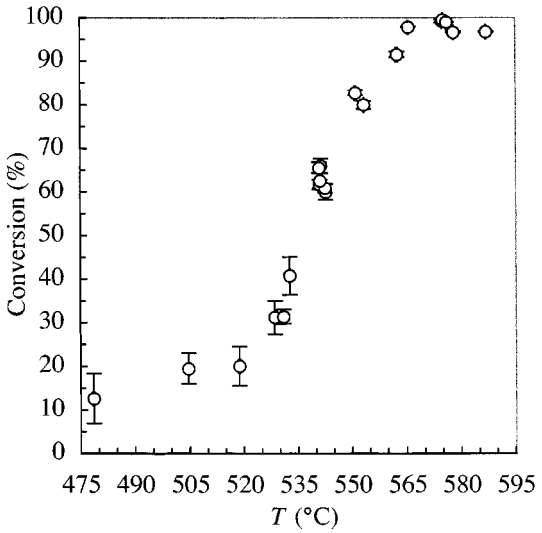

Figure 1. Benzene conversion as a function of temperature.

$\tau = 6.2 \pm 0.4$ s; $P = 246 \pm 2$ bar; $\Phi = 1.1 \pm 0.1$; $[C_6H_6]_0 = 0.60 \pm 0.04$ mM.

$$\text{Carbon fraction} = \frac{\text{Moles of carbon in product}}{\text{Moles of carbon in feed}}. \quad (2)$$

By plotting each product on a carbon basis as defined by Eq. 2, the fate of the carbon in the feed is readily apparent. The total of all product carbon fractions and that of the unreacted benzene sum to one, if all of the carbon in the feed is recovered in effluent.

Table 2. Benzene Oxidation Experiments

Parameter (No. of Exp.)	Parameter	Fixed Conditions	Residence Time
Temperature variation (21)	479–587°C	$[C_6H_6]_0 = 0.6$ mM $\Phi = 1.1$ $P = 246$ bar	6 s
Φ Variation (31 @ 540°C; 11 @ 550°C)	0.5–2.5	$T = 540, 550$°C $[C_6H_6]_0 = 0.6$ mM $P = 246$ bar	3–7 s
$[C_6H_6]_0$ Variation (3 @ 530°C; 24 @ 540°C; 11 @ 550°C)	0.4–1.2 mM	$T = 530, 540, 550$°C $\Phi = 1.0 \pm 0.1$ $P = 246$ bar	6 s @ 530°C 3–7 s @ 540°C 3–7 s @ 550°C
Pressure (density) variation (22)	138–278 bar (0.03–0.09 g/mL)	$T = 540$°C $[C_6H_6]_0 = 0.6$ mM $\Phi = 0.9$	3–6 s

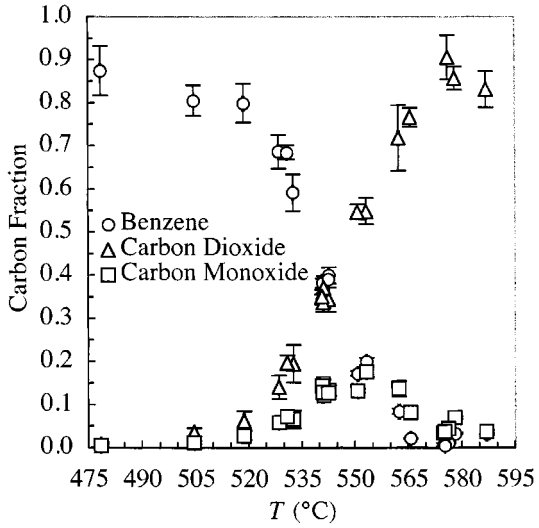

Figure 2. Carbon fractions of carbon dioxide, carbon monoxide, and unreacted benzene as a fuction of temperature.

$\tau = 6.2 \pm 0.4$ s; $P = 246 \pm 2$ bar; $\Phi = 1.1 \pm 0.1$; $[C_6H_6]_0 = 0.60 \pm 0.04$ mM.

Carbon dioxide and carbon monoxide are the oxidation products accounting for the largest amount of reacted carbon. The oxidation of benzene yields more CO_2 than CO at all conditions, which is fully consistent with the SCWO of phenol and substituted phenols as discussed earlier. Even at 479°C, where the benzene conversion is very low, the CO_2 yield was 7.53×10^{-3} mol/mol compared to 4.81×10^{-3} mol/mol for CO. While the carbon fraction of CO_2 continually increases with temperature, that of CO increases only up to 540°C, after which the temperature is sufficient for the oxidation of CO to CO_2. By 575°C, nearly 100% benzene conversion is achieved, with CO_2 accounting for 90% of the carbon in the feed. A study of the electrochemical oxidation of benzene in aqueous bisulfate solutions at 25 to 250°C (Bard et al., 1988) also showed CO_2 to be the major oxidation product at all temperatures. CO was not detected in this investigation.

Methane was the only other gas-phase, carbon-containing product detected in appreciable quantities. Methane accounted for up to 5% of the carbon in the feed. The methane carbon fraction increases with increasing temperature, indicating that methane is not undergoing further oxidation at these conditions.

Several additional light gases were detected. Ethylene, acetylene, and propylene were observed, although in quantities unimportant to the carbon balance. Hydrogen was only found at high temperatures under oxygen-depleted conditions, and was presumably formed via a global water–gas shift pathway. Unreacted benzene was also detected in the gas phase.

Phenol was the only detected liquid-phase product. At most, phenol accounted for 2% of the carbon. Phenol was not detected below 505°C, indicating that phenol is not formed at the lower temperatures where only minimal benzene oxidation occurs. No phenol was detected above 575°C, suggesting that phenol is oxidized at a rate comparable to its rate of formation.

Between 90 and 100% of the carbon in the feed was recovered in the effluent products: CO, CO_2, methane, phenol, trace light hydrocarbon gases, and unreacted benzene. Figure 4 shows a graph of the recovered carbon as a function of temperature, with recovered carbon defined by

$$\text{Recovered carbon} = \frac{\text{Moles of carbon in effluent}}{\text{Moles of carbon in feed}} \times 100\%. \quad (3)$$

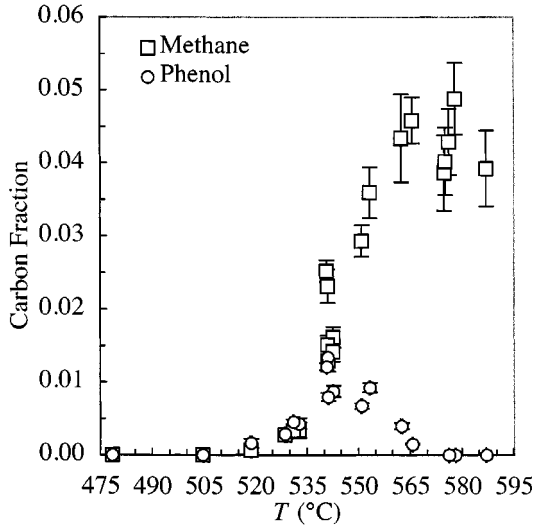

Figure 3. Carbon fractions of methane and phenol as a function of temperature.

$\tau = 6.2 \pm 0.4$ s; $P = 246 \pm 2$ bar; $\Phi = 1.1 \pm 0.1$; $[C_6H_6]_0 = 0.60 \pm 0.04$ mM.

Higher carbon recoveries are observed with higher benzene conversions, as almost all of the reacted carbon is in the form of CO, CO_2, and methane.

Fuel Equivalence Ratio Variations. The fuel equivalence ratio (Φ) was varied from 0.48 (100% excess oxygen) to 2.5 (40% of oxygen demand) at 246 bar and with an initial benzene concentration of 0.6 mM at both 540 and 550°C. Benzene conversion exhibited a pronounced dependence on Φ at both 540°C and 550°C, consistent with the experimental observations for phenol SCWO (Thornton and Savage, 1990; Krajnc and Levec, 1996; Koo et al., 1997). Figure 5 displays these results at 540°C. The lines in the figures indicate trends and are included only for visualization purposes. A dependence on oxygen concentration is not always observed for oxidation in SCW (Holgate and Tester, 1993). The fact that benzene and phenol conversions are functions of Φ signifies that oxygen participates in important radical-generating reactions in their oxidation mechanisms.

With an increasing initial oxygen-to-benzene ratio (decreasing Φ), the proportion of benzene that oxidizes completely to CO_2 also increases. The yields of CO, phenol, and

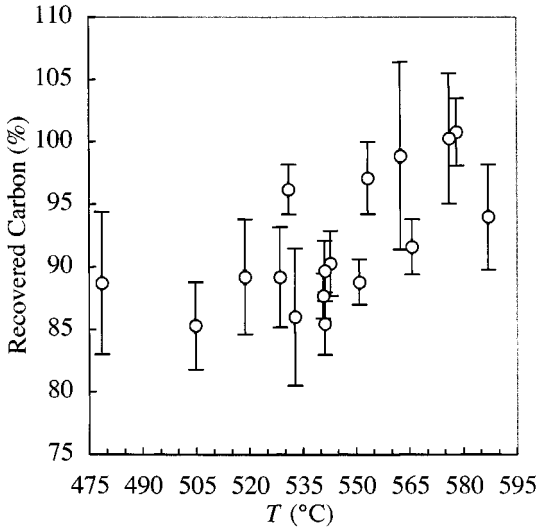

Figure 4. Recovered carbon as a function of temperature.

$\tau = 6.2 \pm 0.4$ s; $P = 246 \pm 2$ bar; $\Phi = 1.1 \pm 0.1$; $[C_6H_6]_0 = 0.60 \pm 0.04$ mM.

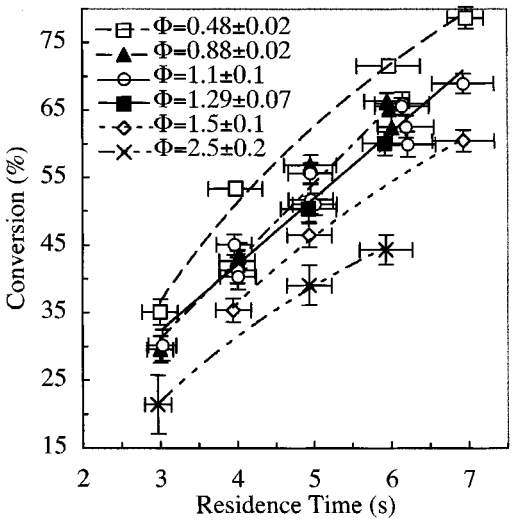

Figure 5. Benzene conversion as a function of residence time and Φ at 540°C.

$T = 540 \pm 2$°C; $P = 246 \pm 2$ bar; $[C_6H_6]_0 = 0.60 \pm 0.04$ mM.

methane, where yield is defined on a reacted carbon basis,

$$\text{Yield} = \frac{\text{Moles carbon in product}}{\text{Moles carbon reacted}}, \qquad (4)$$

decrease with increasing oxygen concentrations fed. Hydrogen is only observed at fuel-rich conditions ($\Phi > 1$), lending support to the previous assumption that the global water–gas shift pathway is the source of hydrogen. At fuel-lean conditions the water–gas shift pathway is not competitive with the non-hydrogen-producing pathway for CO to CO_2 oxidation (Holgate et al., 1992), and hydrogen is not formed. Carbon balances for these experiments, based on the concentrations of phenol, methane, CO, CO_2, and unreacted benzene, were consistently 85 to 95%.

Inlet Benzene Concentration Variations. While maintaining a stoichiometric amount of oxygen and a pressure of 246 bar, experiments were performed with initial benzene concentrations of 0.4, 0.6, and 1.2 mM at 530, 540, and 550°C. As shown in Figure 6, benzene conversion decreases on average 20 to 30% at 540°C, with a doubling of the initial benzene concentration from 0.6 to 1.2 mM. Complementary experiments at 530°C at a 6-s residence time again showed decreasing conversions with increasing initial benzene concentrations. At 550°C, however, the concentration dependence was greatly diminished and not measurable at a statistically significant level. The product yields, defined in Eq. 4, were not found dependent on the initial benzene concentration, indicating that benzene forms products in the same proportions.

Dependence of conversion on the initial feed concentration is a common observation in studies of SCW oxidation kinetics. For example, Holgate and Tester (1993) showed that hydrogen conversion decreased with an increasing initial hydrogen concentration at 550°C with a stoichiometric amount of oxygen. Acetic acid conversion, on the other hand, increased with increasing feed concentration (Meyer et al., 1995). Phenol conversion exhibited no dependence on the feed concentration (Thornton and Savage, 1992a; Krajnc and Levec, 1996). A dependence of conversion on the feed concentration arises from the involvement of the feed in radical generating or radical quenching reactions in the overall free-radical oxidation mechanism. The decrease in conversion with increasing benzene feed concentration suggests that benzene may catalyze the recombination of radicals. As an example of catalysis of radical recombination, consider the following elementary reactions of XH (such as $XH = C_6H_6$) with OH and H radicals:

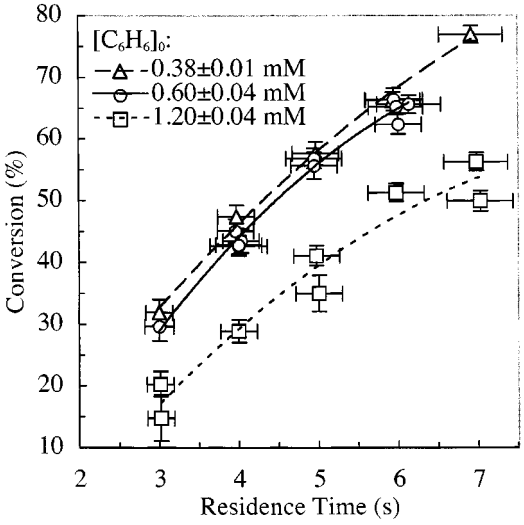

Figure 6. Benzene conversion as a function of residence time and $[C_6H_6]_0$ at 540°C.

$T = 540 \pm 2$°C; $P = 246 \pm 2$ bar; $\Phi = 0.9 \pm 0.1$.

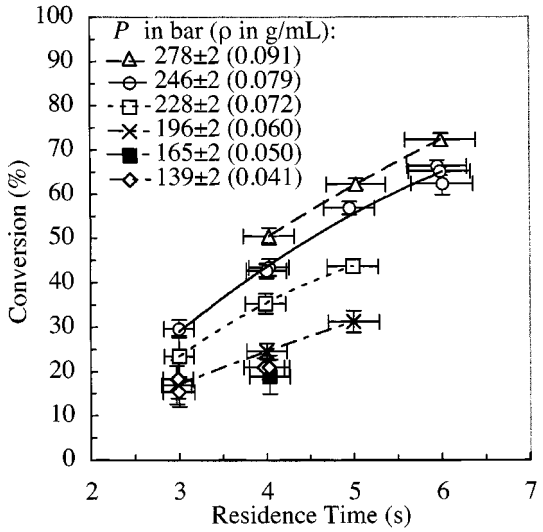

Figure 7. Effect of pressure and residence time on benzene conversion at 540°C.

$T = 540 \pm 2$°C; $[C_6H_6]_0 = 0.60 \pm 0.04$ mM; $\Phi = 0.9 \pm 0.1$.

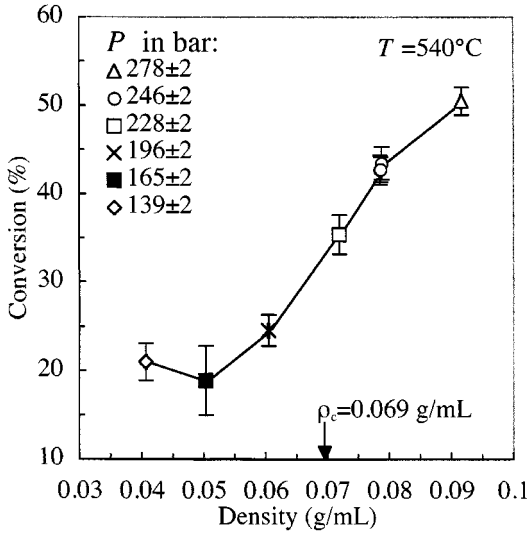

Figure 8. Variation of benzene conversion with density.

$T = 540 \pm 2$°C; $[C_6H_6]_0 = 0.60 \pm 0.04$ mM; $\Phi = 0.9 \pm 0.1$.

$$XH + OH = X + H_2O \qquad (R1)$$

$$X + H = XH. \qquad (R2)$$

If the net forward rate of Eqs. R1 and R2 are positive, the combined effect is the recombination of radicals:

$$OH + H = H_2O \qquad (R1\&R2).$$

The participation of benzene in two or more such reactions where the net effect is the loss of radicals would yield the observed effect. And, if the elementary reactions have different activation energies, and hence different temperature dependencies, the significance of radical quenching effects will vary with temperature, as was observed.

Pressure (Density) Variations. A final set of experiments was performed to ascertain the influence of operating pressure or fluid density on benzene conversion. Pressure was varied from 139 bar to 278 bar at 540°C with a stoichiometric amount of oxygen and an initial benzene concentration of 0.6 mM. The increasing pressure at 540°C produced a corresponding rise in the density from 0.041 g/mL at 139 bar to 0.091 g/mL at 278 bar. Interestingly, as shown in Figure 7, at subcritical pressures ($P_c = 221$ bar) conversion is independent of pressure, while above P_c conversion clearly increases as pressure increases. A positive dependence of conversion on system pressure was also seen during phenol (Thornton and Savage, 1990; Koo et al., 1997) and in hydrogen and carbon monoxide oxidation (Holgate and Tester, 1994a).

In a supercritical water system, increasing pressure also increases the water density (concentration). As a result, it is not apparent which variable, pressure, or water concentration is affecting the benzene reaction rate. Recently, Koo et al. (1997) addressed this issue in the case of phenol oxidation at 400°C with 860% excess oxygen. Using a batch reactor, Koo et al. first measured the oxidation rate as a function of residence time at 223 bar, which corresponds to a water concentration of 6.9 M (0.124 g/mL). Next, the reactor pressure was increased to 253 bar in two ways: first by increasing the water concentration to 9.7 M (0.175 g/mL), and second by maintaining the water concentration at 6.9 M and increasing pressure with the addition of helium. Comparison of the phenol conversion as a function of residence time from the three experiments demonstrated that the increasing water concentration, not the increasing pressure, induced the increase in the reaction rate. In an earlier study, Holgate and Tester (1994b) explored theoretically the dependence of hydrogen and carbon monoxide oxidation rates on pressure using elementary reaction mechanisms; they also concluded that the changing water concentration was the primary source of the apparent pressure dependence. Assuming that the apparent dependence of benzene conversion on pressure or density arises from the increasing water concentration, the 4 s residence time data from Figure 7 is replotted with density as the independent variable in Figure 8. Evaluation of an elementary reaction mechanism for benzene oxidation in SCW lends further support to this assumption (DiNaro et al., 2000).

Regressed Global Rate Expression

A global rate expression was regressed from the experimental data as a means of conveniently representing the benzene oxidation rate over the conditions studied. Based on the assumption that the reactor behaves as an ideal isothermal, isobaric plug-flow reactor, the reaction rate should obey the plug-flow design equation:

$$\frac{\tau}{C_{i,0}} = \int_0^{X_i} \frac{dX_i}{-R_i}, \qquad (5)$$

where τ is the residence time, $C_{i,0}$ is the initial concentration of reactant i, X_i is the measured conversion of species i, and R_i is the reaction rate for species i. The form of the global

rate expression that was selected to represent the oxidation of benzene is given by:

$$-R_i = -\frac{d[C_6H_6]}{dt} = A\exp(-E_a/RT)[C_6H_6]^a[O_2]^b[H_2O]^c, \quad (6)$$

where A is the preexponential factor, E_a the activation energy, and a, b, and c are the reaction orders with respect to benzene, oxygen, and water, respectively. Rewriting $[C_6H_6]$ and $[O_2]$ in terms of X and inserting Eq. 6 into Eq. 5 results in the following expression for an isothermal experiment:

$$k\tau[C_6H_6]_0^{a+b-1}[H_2O]^c = \int_0^X \frac{dX}{(1-X)^a(\phi - 7.5X)^b}, \quad (7)$$

where

$$k = A\exp(-E_a/RT); \qquad \phi = [O_2]_0/[C_6H_6]_0. \quad (8)$$

Since the reacting mixture is very dilute (< 0.1 wt. % C_6H_6), water concentration remains essentially constant during an experiment allowing the water concentration to be moved outside of the integral. Notably, use of the stoichiometric oxygen-to-benzene ratio in Eq. 7 is based on the assumption that all reacted benzene undergoes complete oxidation to CO_2 and water. While this assumption is not completely accurate, as partial oxidation products, mostly CO and some phenol and methane, were detected in the effluent, using the stoichiometric ratio as a correlating parameter is reasonable, since CO_2 was always the highest yielding product.

A nonlinear regression of all experimental data was performed in order to determine A, E_a, a, b, and c in Eq. 6 and resulted in the following best-fit global rate expression for benzene oxidation in SCW:

$$-\frac{d[C_6H_6]}{dt} = 10^{13.7\pm1.0}\exp(-2.7\pm0.1\times10^5/RT) \times [C_6H_6]^{0.40\pm0.07}[O_2]^{0.17\pm0.05}[H_2O]^{1.4\pm0.1}. \quad (9)$$

This expression can be used to calculate the benzene oxidation rate in SCW within the range of the predictions over which it was regressed. The units of the parameter are J, mol, L, s. The parameter uncertainties are calculated at the 95% confidence level. The regression returned a reaction order with respect to benzene significantly less than 1 and a nonzero reaction order with respect to oxygen. For comparison, in three separate studies of phenol SCWO (Gopalan and Savage, 1995; Krajnc and Levec, 1996; Koo et al., 1997) the reaction order with respect to phenol was found to be approximately unity. The regressed parameters are not very sensitive to the value used for the oxygen-to-benzene ratio in Eq. 7. For example, using 6.5 instead of 7.5 for this ratio (a 13% decrease) yields only a 1.5% decrease in E_a, a 2.2% decrease in A, no change in a or c, and an 8% increase in b. Since the regressed parameters are correlated and their numerical values also depend upon the regression routine used, care should be taken when directly comparing parameters, especially A and E_a, with the results from other research groups. A better test of data consistency is a one-to-one comparison of predicted to experimental conversions.

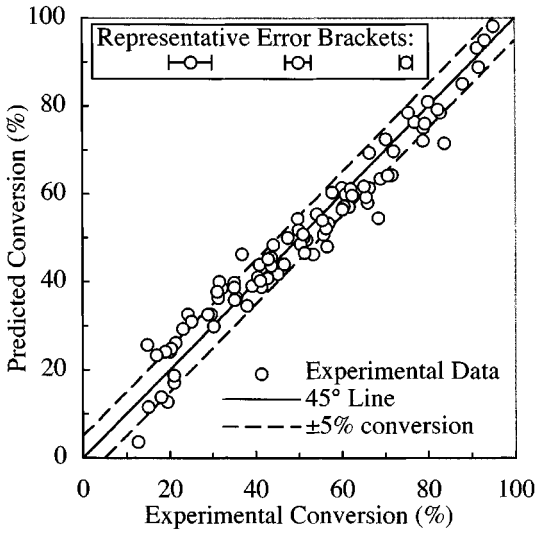

Figure 9. Experimental conversion vs. predictions of the regressed global rate expression.

The representative error brackets indicate the average error in measured conversion at $X = 25$, 50, and 75%. $T = 479-587$°C; $\tau = 3-7$ s; $P = 139-278$ bar; $[C_6H_6]_0 = 0.4-1.2$ mM, $\Phi = 0.5-2.5$.

Figure 9 compares the predicted and experimental benzene conversion. Predicted conversion is plotted along the Y- and experimental conversion along the X-axis. The "Representative Error Brackets" in Figure 9 show the average error in measured conversion at the 95% confidence level at 25, 50, and 75% conversion. Generally, high-conversion measurements are more accurate than those at low conversion. Most of the data lie within ± 5% conversion of the "perfectly matched" 45° line, indicating that Eq. 9 represents benzene oxidation at the studied experimental conditions ($T = 479-587$°C, $P = 139-278$ bar, $[C_6H_6]_0 = 0.4-1.2$ mM, $\Phi = 0.5-2.5$, and $\tau = 3-7$ s) and suggests internal consistency among the data. The largest discrepancies between model predictions and data are at benzene conversions of less than 35% and mostly correspond to short residence-time data ($\tau = 3-4$ s) at various conditions. Since benzene conversion exceeded 35% in a majority of the experiments, the parameters in Eq. 9 are weighted to better represent higher-conversion data. However, taking into account the higher level of uncertainty in the low-conversion data, the model predictions are generally in equally good agreement with the low- and high-conversion data. The two drastically underpredicted, low-conversion points in Figure 9 correspond to the measurements at 478 and 505°C from Figure 1. Here the predicted conversions may be more accurate than those measured.

Formation of Single- and Multi-ringed Aromatic Species

A common observation among researchers studying the oxidation kinetics of phenol and substituted phenols was the

Table 3. Experiments Conducted for the Detection of Single- and Multiringed Aromatic Products

Run No.	Temp. (°C)	Φ	Conv. (%)	Carbon Balance (%)
632	577	1.2 ± 0.3	92.4 ± 0.6	102 ± 5
633	528	1.1 ± 0.4	23 ± 4	89 ± 4
636	625	1.0 ± 0.3	95.4 ± 0.3	102 ± 5
637	625	1.3 ± 0.3	90.9 ± 0.6	94 ± 4
638	625	0.9 ± 0.3	98.4 ± 0.1	97 ± 5

Note: $\tau = 6.0 \pm 0.1$ s; $P = 246 \pm 2$ bar; $[C_6H_6]_0 = 0.50 \pm 0.02$ mM.

formation of dimers and single-ring aromatic species (such as Thornton and Savage, 1990 or Krajnc and Levec, 1996). The formation of such products depended on the reactor conditions and appeared more abundant at lower temperatures and with lower oxygen levels. Based on the carbon balances in the oxidation experiments of this study, benzene oxidizes to form primarily CO, CO_2, phenol, and methane at the conditions listed in Tables 1 and 2. In fact, at temperatures above 575°C with stoichiometric oxygen benzene undergoes near-complete conversion to CO_2 and any additional, undetected partial oxidation products, including organic acids, dimers, and single-ring aromatic species, will only constitute a very minor fraction of the reacted carbon (< 1 mol %).

Five experiments were conducted for the purpose of searching for single- and multi-ringed aromatic products and monitoring their occurrence as a function of temperature and the initial oxygen concentration. The experimental conditions, measured benzene conversions, and calculated carbon balances based on the effluent concentrations of CO, CO_2, methane, phenol, and unreacted benzene are shown in Table 3. These experiments were conducted before undertaking the detailed investigation of benzene oxidation kinetics summarized earlier and were performed in an 8-m × 1/8-in. (3.2-mm) OD × 0.046-in. (1.2-mm) ID 316SS reactor. Otherwise, the reactor system was identical to that used for the reported benzene oxidation experiments. The measured benzene conversions and product yields were fully consistent with those observed in the 4.71-m reactor.

Table 4 lists the most prevalent partial oxidation products. Those products labeled ''positively identified'' were identified both by matching the product mass-spectra with library spectra and their retention times to those of standards. Since standards were not available for those species in column two, they were identified by mass-spectra matches only, and their identities must be considered tentative.

The GC/MS was calibrated for the six compounds listed in column one of Table 4 using purchased analytical standards.

Table 4. Single- and Multi-ringed Aromatic Partial Oxidation Products Identified by GC/MS Analysis of the Concentrated Effluent

Positively* Identified Products	Tentatively** Identified Products
Styrene	Benzaldehyde
Acetophenone	*p*-Benzoquinone
Biphenyl	Benzofuran
Napththalene	2,3 Dihydro-1*H*-Inden-1-one
Dibenzofuran	9*H*-Fluoren-9-one
Anthracene	Xanthone

*Identified both by mass-spectrum and retention-time match.
**Identified by mass-spectrum match only.

Table 5. Absolute Concentrations of the Single- and Multiringed Intermediates

Run No. (Conditions)	Conc. of Single- and Multiringed Products (mol/mL)	Initial Carbon Accounted for by Sum of all Single- and Multiringed Products (%)
633 (528°C, Φ = 1.1)	10^{-9}–10^{-11}	0.2
632 (577°C, Φ = 1.2)	10^{-10}–10^{-12}	2.0
636 (625°C, Φ = 1.0)	10^{-10}–10^{-12}	0.3
637 (625°C, Φ = 1.3)	10^{-11}–10^{-13}	0.1
638 (625°C, Φ = 0.9)	10^{-11}–10^{-13}	0.02

Note: $\tau = 6.0 \pm 0.1$ s; $P = 246 \pm 2$ bar; $[C_6H_6]_0 = 0.50 \pm 0.02$ mM.

To estimate concentrations of the compounds listed in column two, the average response factor (RF) of styrene and acetophenone was used as the RF for the single-ringed aromatics, and the average RF of biphenyl, naphthalene, dibenzofuran, and acetophenone used as the RF for the multiringed aromatics.

Quantification of the analytes was performed by measuring the concentration of each species in the extracted, concentrated sample and then back-calculating their concentrations in the reactor, assuming no loss of analytes during sample preparation. The ranges of the absolute concentrations of the single- and multi-ringed aromatic species are shown in Table 5. Also shown are the total contribution of all single- and mult-iringed species to the carbon balance in each experiment. One should note that the species concentrations and carbon balance contributions are only approximate, as some of the analytes may have been lost during sample preparation. Without accounting for sample loss, at 625°C with excess oxygen, less than 0.1% of the initial carbon is present in the form of single- and multi-ringed products. The concentrations of the nonoxygenated species, such as the soot-precursors styrene, naphthalene, and anthracene formed by the addition of acetylene to the benzene ring, decreased substantially with excess oxygen. The concentrations of all oxygenated intermediates decreased with both increasing temperature and oxygen concentration and, with the exception of xanthone and dibenzofuran, were undetectable at reaction temperatures of 625°C with excess oxygen present. Dibenzofuran and xanthone are structurally similar, as they consist of two aromatic rings joined by an O atom. Of particular interest is the presence of *p*-benzoquinone, which was also observed in the SCWO of phenol and substituted phenols (Thornton and Savage, 1990; Krajnc and Levec, 1997). Dibenzofuran and biphenyl were the most persistent and among the highest concentration single- and multiringed species at all conditions listed in Table 3.

Conclusions

A total of seven hydrolysis and 107 oxidation experiments were conducted to characterize the reactivity of benzene in supercritical water. Since the conversion of benzene in the absence of oxygen was determined to be no greater than 10% and realistically closer to 2% at temperatures up to 625°C, the hydrolysis pathway did not interfere with the characteri-

zation of oxidation kinetics. Essentially, complete conversion of benzene was achieved at 575°C and 246 bar with a stoichiometric amount of oxygen, and carbon dioxide accounted for 90% of the initial carbon. Benzene conversion by oxidation increased with both increasing oxygen concentration and system pressure. While at 530 and 540°C the benzene oxidation rate decreased with increasing initial benzene concentrations, at 550°C no significant dependence of conversion on the initial concentration existed. At a 95% confidence level, a regressed global rate expression was developed with an activation energy of 240 ± 10 kJ/mol and orders with respect to benzene, oxygen, and water of 0.40 ± 0.07, 0.17 ± 0.05, and 1.4 ± 0.1, respectively. This empirical model represents benzene oxidation at most of the studied experimental conditions to within $\pm 5\%$ conversion.

More than 90% of the carbon in the reactor feed was recovered in the effluent products. Carbon dioxide accounted for more of the reacted carbon than any other oxidation product, including carbon monoxide, at all reactor conditions and for all levels of benzene conversion. Methane and phenol were also dominant oxidation products. Trace levels of ethylene, acetylene, and propylene were detected. Single- and multiringed aromatic products were also detected in the effluent. Their concentrations decreased significantly, many to undetectable levels, as both the temperature and oxygen concentration were increased. At 625°C and with 10% excess oxygen, less than 0.1% of the initial carbon was present in the form of single- and multi-ringed products. Dibenzofuran and biphenyl were the most persistent of the single- and multiringed intermediates. Similar to the case of oxidation of phenol and substituted phenols in supercritical water, *p*-benzoquinone was also detected in the effluent.

Acknowledgment

The authors gratefully acknowledge the partial support of the Army Research Office through its University Research Initiative (Grant No. DAAL03-92-G-0177) and AASERT Programs (Grant No. DAAH04-94-G-0145), both under the supervision of Dr. Robert Shaw, Sandia National Laboratories through its Strategic Environmental Research and Development Program (SERDP) under the direction of Dr. Steven Rice, and the NIEHS Superfund program. We also thank Dr. Art LaFleur, Dr. Koli Taghizadeh, Ms. Elaine Plummer, and Mr. John LoRusso of the MIT Core Analytical Laboratory for the use of the analytical instruments and technical assistance. In addition, we thank Professors Kenneth Smith and Paul Laibinis, Dr. William Peters, and the other current and former members of the MIT SCWO research group.

Literature Cited

Aki, S., and M. A. Abraham, "Catalytic Supercritical Water Oxidation of Pyridine: Comparison of Catalysts," *Ind. Eng. Chem. Res.*, **38**, 358 (1999).

Bard, A. J., W. M. Flarsheim, and K. P. Johnston, "High-Pressure Eletrochemical Oxidation of Benzene at a Lead Dioxide Electrode in Aqueous Bisulfate Solutions at 25° to 250°C," *J. Electrochem. Soc.*, **135**, 1939 (1988).

Crain, N., S. Tebbal, L. Li, and E. F. Gloyna, "Kinetics and Reaction Pathways of Pyridine Oxidation in Supercritical Water," *Ind. Eng. Chem. Res.*, **32**, 2259 (1993).

DiNaro, J. L., "Oxidation of Benzene in Supercritical Water: Experimental Measurements and Development of an Elementary Reaction Mechanism," PhD Thesis, Dept. of Chemical Engineering, Massachusetts Institute of Technology, Cambridge (1999).

DiNaro, J. L., J. B. Howard, W. H. Green, J. W. Tester, and J. W. Bozzelli, "Analysis of an Elementary Reaction Mechanism for Benzene Oxidation in Supercritical Water," *Proc. 28th Symp. (Intl.) on Combustion* (2000).

Ding, Z. Y., S. N. V. K. Aki, and M. A. Abraham, "Catalytic Supercritical Water Oxidation: An Approach for Complete Destruction of Aromatic Compounds," *Innovations in Supercritical Fluids: Science and Technology*, K. W. Hutchenson and N. Foster, eds., ACS Symposium Series, Vol. 608, American Chemical Society, Washington, DC, p. 232 (1995a).

Ding, Z. Y., S. N. V. K. Aki, and M. A. Abraham, "Catalytic Supercritical Water Oxidation: Phenol Conversion and Product Selectivity," *Environ. Sci. Technol.*, **29**, 2748 (1995b).

Glyona, E. F., and L. Li, "Supercritical Water Oxidation Research and Development Update," *Environ Prog.*, **14**, 182 (1995).

Gopalan, S., and P. E. Savage, "A Reaction Network Model for Phenol Oxidation in Supercritical Water," *AIChE J.*, **41**, 1864 (1995).

Helling, R. K., and J. W. Tester, "Oxidation Kinetics of Carbon Monoxide in Supercritical Water," *Energy Fuels*, **4**, 417 (1987).

Helling, R. K., and J. W. Tester, "Oxidation of Simple Compounds and Mixtures in Supercritical Water: Carbon Monoxide, Ammonia and Ethanol," *Environ. Sci. Technol.*, **22**, 1319 (1988).

Holgate, H. R., J. C. Meyer, and J. W. Tester, "Glucose Hydrolysis and Oxidation in Supercritical Water.," *AIChE J.*, **41**, 637 (1995).

Holgate, H. R., and J. W. Tester, "Fundamental Kinetics and Mechanisms of Hydrogen Oxidation in Supercritical Water," *Combust. Sci. Technol.*, **88**, 369 (1993).

Holgate, H. R., and J. W. Tester, "Oxidation of Hydrogen and Carbon Monoxide in Sub- and Supercritical Water: Reaction Kinetics, Pathways, and Water-Density Effects: 1. Experimental Results," *J. Phys. Chem.*, **98**, 800 (1994a).

Holgate, H. R., and J. W. Tester, "Oxidation of Hydrogen and Carbon Monoxide in Sub- and Supercritical Water: Reaction Kinetics, Pathways, and Water-Density Effects: 2. Elementary Reaction Modeling," *J. Phys. Chem.*, **98**, 810 (1994b).

Holgate, H. R., P. A. Webley, J. W. Tester, and R. K. Helling, "Carbon Monoxide Oxidation in Supercritical Water: The Effects of Heat Transfer and the Water-Gas Shift Reaction on Observed Kinetics," *Energy Fuels*, **6**, 586 (1992).

Jin, L., Z. Y. Ding, and M. A. Abraham, "Catalytic Supercritical Water Oxidation of 1,4-Dichlorobenzene," *Chem. Eng. Sci.*, **47**, 2659 (1992).

Killilea, W. R., and K. C. Swallow, "The Fate of Nitrogen in Supercritical Water Oxidation," *J. Supercrit. Fluids*, **5**, 72 (1992).

Koo, M., W. K. Lee, and C. H. Lee, "New Reactor System for Supercritical Water Oxidation and Its Application on Phenol Destruction," *Chem. Eng. Sci.*, **52**, 1201 (1997).

Krajnc, M., and J. Levec, "On the Kinetics of Phenol Oxidation in Supercritical Water," *AIChE J.*, **42**, 1977 (1996).

Krajnc, M., and J. Levec, "Oxidation of Phenol Over a Transition-Metal Oxide Catalyst in Supercritical Water," *Ind. Eng. Chem. Res.*, **36**, 3439 (1997).

Lachance, R., J. Paschkewitz, J. DiNaro, and J. W. Tester, "Thiodiglycol Hydrolysis and Oxidation in Sub- and Supercritical Water," *J. Supercrit. Fluids*, **16**, 133 (1999).

Li, R., T. D. Thornton, and P. E. Savage, "Kinetics of CO_2 Formation from the Oxidation of Phenols in Supercritical Water," *Environ. Sci. Technol.*, **26**, 2388 (1992).

Marrone, P. A., T. A. Arias, W. A. Peters, and J. W. Tester, "Solvation Effects on Kinetics of Methylene Chloride Reactions in Sub- and Supercritical Water: Theory, Experiment, and *ab initio* Calculations," *J. Phys. Chem.*, **102**, 7013 (1998a).

Marrone, P. A., P. M. Gschwend, W. A. Peters, and J. W. Tester, "Product Distribution and Reaction Pathways for Methylene Chloride Hydrolysis and Oxidation Under Hydrothermal Conditions," *J. Supercrit. Fluids*, **12**, 239 (1998b).

Marrone, P. A., R. P. Lachance, J. L. DiNaro, B. D. Phenix, J. C. Meyer, J. W. Tester, W. A. Peters, and K. C. Swallow, "Methylene Chloride Oxidation and Hydrolysis in Supercritical Water," *Innovations in Supercritical Fluids: Science and Technology*, chap. 13, K. W. Hutchenson and N. Foster, eds., ACS Symp. Ser., Vol. 608 (1995).

Martino, C. J., and P. E. Savage, "Supercritical Water Oxidation Kinetics, Products, and Pathways for CH_3- and CHO-Substituted Phenols," *Ind. Eng. Chem. Res.*, **36**, 1391 (1997).

Martino, C. J., and P. E. Savage, "Oxidation and Thermolysis of

Methoxy-, Nitro-, and Hydroxy-Substituted Phenols in Supercritical Water,'' *Ind. Eng. Chem. Res.*, **38**, 1784 (1999a).
Martino, C. J., and P. E. Savage, ''Supercritical Water Oxidation Kinetics and Pathways for Ethylphenols, Hydroxyacetophenones, and Other Monosubstituted Phenols,'' *Ind. Eng. Chem. Res.*, **38**, 1775 (1999b).
Martino, C. J., P. E. Savage, and J. Kasiborski, ''Kinetics and Products from *o*-Cresol Oxidation in Supercritical Water,'' *Ind. Eng. Chem. Res.*, **34**, 1941 (1995).
Meyer, J. C., P. A. Marrone, and J. W. Tester, ''Acetic Acid Oxidation and Hydrolysis in Supercritical Water,'' *AIChE J.*, **41**, 2108 (1995).
Modell, M., ''Supercritical Water Oxidation,'' *Standard Handbook of Hazardous Waste Treatment and Disposal*, H. M. Freeman, ed., McGraw-Hill, New York, p. 8.153 (1989).
Oshima, Y., K. Hori, M. Toda, T. Chommanad, and S. Koda, ''Phenol Oxidation Kinetics in Supercritical Water,'' *J. Supercrit. Fluids*, **13**, 241 (1998).
Phenix, B., J. DiNaro, J. Tester, J. Howard, and K. Smith, ''The Effects of Mixing and Oxidant Choice in Laboratory-Scale Measurements of Supercritical Water Oxidation Kinetics,'' *Ind. Eng. Chem. Res.* to be submitted (2001).
Rice, S. F., and R. R. Steeper, ''Oxidation Rates of Common Organic Compounds in Supercritical Water,'' *J. Hazard. Mater.*, **59**, 261 (1998).
Salvatierra, D., J. D. Taylor, P. A. Marrone, and J. W. Tester, ''Kinetic Study of Hydrolysis of Methylene Chloride from 100 to 500°C,'' *Ind. Eng. Chem. Res.*, **38**, 4169 (1999).
Savage, P. E., ''Organic Chemical Reactions in Supercritical Water,'' *Chem. Rev.*, **99**, 603 (1999).
Savage, P. E., S. Gopalan, T. I. Mizan, C. J. Martino, and E. E. Brock, ''Reactions at Supercritical Conditions: Applications and Fundamentals,'' *AIChE J.*, **41**, 1723 (1995).
Tester, J. W., and J. A. Cline, ''Hydrolysis and Oxidation in Sub- and Supercritical Water: Connecting Process Engineering Science to Molecular Interactions,'' *Corrosion*, **55**, 1088 (1999).
Tester, J. W., H. R. Holgate, F. J. Armellini, P. A. Webley, W. E. Killilea, G. T. Hong, and H. E. Barner, ''Supercritical Water Oxidation Technology: A Review of Process Development and Fundamental Research,'' *Emerging Technologies for Hazardous Waste Management*, Vol. III, Chap. 3, D. W. Tedder and F. G. Pohland, eds., ACS Symp. Ser., Vol. 518 (1993a).
Tester, J. W., P. A. Webley, and H. R. Holgate, ''Revised Global Kinetic Measurments of Methanol Oxidation in Supercritical Water,'' *Ind. Eng. Chem. Res.*, **32**, 236 (1993b).
Thammanayakatip, C., Y. Oshima, and S. Koda, ''Inhibition Effect in Supercritical Water Oxidation of Hydroquinone,'' *Ind. Eng. Chem. Res.*, **37**, 2061 (1998).
Thomason, T. B., G. T. Hong, K. C. Swallow, and W. R. Killilea, ''The MODAR Supercritical Water Oxidation Process,'' *Innovative Hazardous Waste Treatment Technology Series*, Vol. 1: *Thermal Processes*, H. M. Freeman, ed., Technomic, Lancaster, PA, p. 31 (1990).
Thornton, T. D., D. E. LaDue III, and P. E. Savage, ''Phenol Oxidation in Supercritical Water: Formation of Dibenzofuran, Dibenzo-*p*-Dioxin, and Related Compounds,'' *Environ. Sci. Technol.*, **25**, 1507 (1991).
Thornton, T. D., and P. E. Savage, ''Phenol Oxidation in Supercritical Water,'' *J. Supercrit. Fluids*, **3**, 240 (1990).
Thornton, T. D., and P. E. Savage, ''Kinetics of Phenol Oxidation in Supercritical Water,'' *AIChE J.*, **38**, 321 (1992a).
Thornton, T. D., and P. E. Savage, ''Phenol Oxidation Pathways in Supercritical Water,'' *Ind. Eng. Chem. Res.*, **31**, 2451 (1992b).
U. S. EPA, *Test Methods for Evaluating Solid Waste*, SW 846, U.S. EPA, Office of Solid Waste and Emergency Response, Washington, DC (1986).
Vogel, F., B. Phenix, J. DiNaro, P. Marrone, S. Rice, W. Peters, J. Howard, and J. Tester, ''Comparison of Experimental Kinetic Measurements of Methanol Oxidation in Supercritcal Water,'' AIChE Meeting, Los Angeles, submitted to *Ind. Eng. Chem. Res.* (2000).
Webley, P. A., H. R. Holgate, D. M. Stevenson, and J. W. Tester, ''Oxidation Kinetics of Model Compounds of Human Metabolic Waste in Supercritical Water,'' *Proc. Int. Conf. on Environmental Systems*, Williamsburg, VA (1990).
Webley, P. A., and J. W. Tester, ''Fundamental Kinetics of Methanol Oxidation in Supercritical Water,'' *Supercritical Fluid Science and Technology*, K. P. Johnston and J. M. L. Penninger, eds., ACS Symp. Ser., Vol. 406, p. 259 (1989).
Webley, P. A., and J. W. Tester, ''Fundamental Kinetics of Methane Oxidation in Supercritical Water,'' *Energy Fuels*, **5**, 411 (1991).
Webley, P. A., J. W. Tester, and H. R. Holgate, ''Oxidation Kinetics of Ammonia and Ammonia-Methanol Mixtures in Supercritical Water in the Temperature Range 530–700° C at 246 bar,'' *Ind. Eng. Chem. Res.*, **30**, 1745 (1991).
Yang, H. H., and C. A. Eckert, ''Homogeneous Catalysis in the Oxidation of *p*-Chlorophenol in Supercritical Water,'' *Ind. Eng. Chem. Res.*, **27**, 2009 (1988).

Manuscript received Nov. 8, 1999, and revision received May 8, 2000.